ELSEVIER

www.elsevier.nl/locate/jorganchem

Journal of Organometallic Chemistry 597 (2000) 164–174

Journal of Organometallic Chemistry

X-ray structure and fluxional behaviour of *N,N′*-di-*p*-fluorophenyltriazenido complex of nickel(II)

A.S. Peregudov *, D.N. Kravtsov, G.I. Drogunova, Z.A. Starikova, A.I. Yanovsky

Institute of Organo-Element Compounds, RAS, 28 Vavilov Street, Moscow, Russia

Received 20 April 1999; received in revised form 2 November 1999

Dedicated in honour of Professor Stanisław Pasynkiewicz on the occasion of his 70th birthday.

Abstract

The Ni(II) triazenide complex, *trans*-(*o*-Tol)Ni(PEt_3)$_2$$N_3Ar_2$ (Ar = *p*-FC_6H_4) (**1**), was synthesized by the reaction of *trans*-(*o*-Tol)Ni(PEt_3)$_2$Br with Ar_2N_3Na. The crystal structure as well as the ^{1}H-, ^{19}F- and ^{31}P-NMR spectra in toluene-d_8 at different temperatures are reported. It was found that the triazenido group acts as a monodentate ligand. Complex **1** in solid state has a *S-cis*-structure with Ni–N(3) σ-bond and exists as a 3:1 mixture of two isomers with *cisoid* or *transoid* orientation of the Me group of the *o*-tolyl ligand relative to the N(1)=N(2) bond. It was established that the *N,N′*-migration of (*o*-Tol)Ni(PEt_3)$_2$ group occurs in a solution of **1**. The migration rate increases with the temperature increase in the range from −104 to −45°C. However, a further increase in the temperature slows down the process. © 2000 Elsevier Science S.A. All rights reserved.

Keywords: Nickel complexes; Triazenido complexes; X-ray structure; Molecular dynamics

1. Introduction

The variety of possible modes of metal coordination with triazenido ligands in triazene complexes was the focus of several studies of the structure of these compounds. However, in the available literature data, the triazenido group most frequently acts as either a bridging ligand between two metal centres (I) or as a bidentate group (II) [1–9]. The monodentate form (III) has until now eluded structural characterization [10–15]:

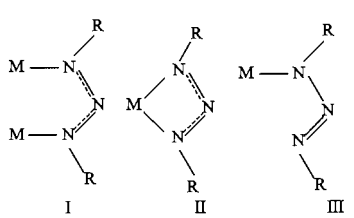

At the same time, the structure (III) may be of particular interest because in such tautomeric systems the N(3)–N(1) σ,σ-migration of ML_n group is possible:

Processes of this kind have been observed in Pd and Pt complexes [13,16], as well as in related Hg and Au triazenides [17–21]. In these cases, relatively easily available compounds with R = Ar and univalent metal-containing groups ML_n were most commonly used as convenient model systems. For some of these complexes the X-ray data suggest the monodentate mode of coordination (III) [10,12,13]. However, up to now there have been practically no data on the structure of diaryltriazenido nickel complexes. In fact, the structures of only two triazenido Ni complexes, Ni_2L_4 (L = PhN_3Ph) [5] and $Ni_2(OH)_2(L')_2(L'')$ (L′ = Ph–N_3H–C_6H_4–N_3H–Ph, L″ = Ph–N_3–$C_6H_4N_3$–Ph), have been studied in solid state [8]. The structures of these bimetallic complexes in solution have not been discussed.

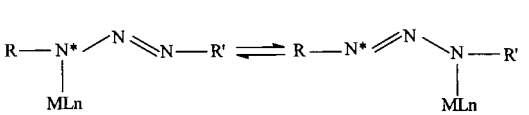

In a previous paper [22], we reported the study of the structure of *N,N′*-di-*p*-fluorophenyltriazenido complex of platinum(II), *trans*-(*o*-Tol)Pt(PEt_3)$_2$$N_3$($C_6H_4F$-*p*)$_2$ (**2**), by dynamic NMR. It has been found that the

* Corresponding author. Fax: +7-095-1355085.
E-mail address: asp@ineos.ac.ru (A.S. Peregudov)

PII: S0022-328X(99)00684-1

above-mentioned migration of the *trans*-(*o*-Tol)-$Pt(PEt_3)_2$ group indeed occurs on the NMR time scale in toluene-d_8 solution:

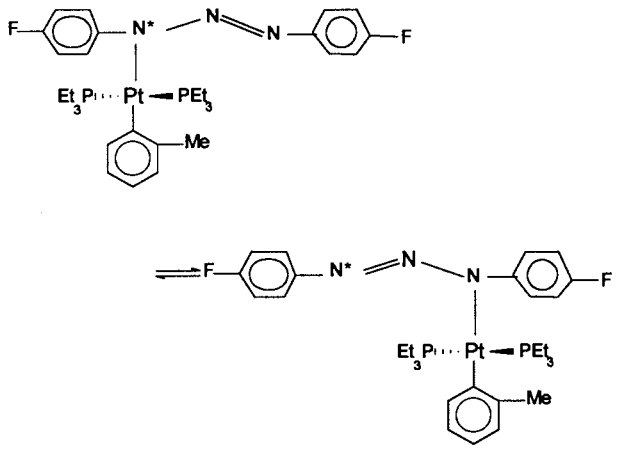

In the present paper, the related complex of Ni(II) was synthesized and its crystal structure, as well as the ^{1}H-, ^{19}F- and ^{31}P-NMR spectra at various temperatures, were studied.

2. Experimental

2.1. Synthesis of trans-(o-Tol)Ni(PEt_3)$_2$$N_3$($C_6H_4$F-p)$_2$ (1)

The starting *N*,*N*′-(di-*p*-fluorophenyl)triazene (DFPT) and *trans*-(*o*-Tol)Ni(PEt_3)$_2$Br (**3**) were prepared according to published procedures [19,23]. A solution of DFPT in methanol was added to a methanol solution of MeONa (1 mmol Na in 10 ml methanol) and after 10 min of stirring, the solution of 1.1 mmol of **3** in the same solvent was added to the reaction mixture. The reaction mixture was stirred for 3 h, the solvent was evaporated, the solid residue washed with water, dried in vacuum and recrystallized from methanol. Yellow solids of **1** (yield 40%) were obtained, m.p. 135–138°C. Anal. Calc. for $C_{31}H_{45}N_3NiP_2F_2$ (**1**): % C, 60.14 (60.21); % H, 7.35 (7.33); % N, 6.82 (6.80).

Table 1
Selected bond lengths (Å) and bond angles (°) for **1**

Bond lengths			
Ni(1)–C(25)	1.924(6)	N(1)–C(19)	1.403(8)
Ni(1)–N(3)	1.943(4)	N(2)–N(3)	1.326(7)
Ni(1)–P(1)	2.220(2)	N(3)–C(13)	1.421(8)
Ni(1)–P(2)	2.221(2)	F(1)–C(22)	1.373(9)
P(1)–C(1)	1.829(7)	F(2)–C(16)	1.377(9)
P(1)–C(5)	1.830(7)	C(1)–C(2)	1.560(11)
P(1)–C(3)	1.847(7)	C(3)–C(4)	1.542(11)
P(2)–C(9)	1.836(7)	C(5)–C(6)	1.533(11)
P(2)–C(7)	1.843(7)	C(7)–C(8)	1.529(11)
P(2)–C(11)	1.851(7)	C(9)–C(10)	1.532(11)
N(1)–N(2)	1.298(7)	C(11)–C(12)	1.486(11)
Bond angles			
C(25)–Ni(1)–N(3)	178.5(3)	N(1)–N(2)–N(3)	110.1(4)
C(25)–Ni(1)–P(1)	86.9(2)	N(2)–N(3)–C(13)	112.8(4)
N(3)–Ni(1)–P(1)	93.1(2)	N(2)–N(3)–Ni(1)	120.5(4)
C(25)–Ni(1)–P(2)	89.7(2)	C(13)–N(3)–Ni(1)	126.5(4)
N(3)–Ni(1)–P(2)	90.4(2)	C(2)–C(1)–P(1)	115.6(5)
P(1)–Ni(1)–P(2)	174.80(7)	C(4)–C(3)–P(1)	115.2(5)
C(1)–P(1)–C(5)	104.9(3)	C(6)–C(5)–P(1)	116.3(5)

2.2. X-ray crystal structure determination

Crystals of **1** are monoclinic; at −78°C, a = 10.499(4), b = 35.24(2), c = 9.143(3) Å, β = 108.76(3)°, V = 3203(2) Å^3, space group $P2_1/c$, Z = 4, $D_{calc.}$ = 1.282 g cm^{-3}, $F(000)$ = 1272.

The data for a greenish–blue crystal having approximate dimensions of 0.2 × 0.2 × 0.5 mm were collected at −78°C on a Syntex $P2_1$ diffractometer using the $\theta/2\theta$ scan mode (θ range 2.0–25.0°). A total of 4976 reflections were averaged to produce 4652 unique data. The structure was solved by the direct method and refined by the least-squares technique in the anisotropic approximation for all non-hydrogen atoms, with the exception of the carbon atoms of the disordered Ph ring of the *o*-tolyl ligand (see Section 3). The H atoms apart from those of the Me groups (at the C(4) and C(12) atoms) of two Et substituents (which were placed geometrically and included in the refinement in the riding model approximation) were located in the difference Fourier synthesis and refined isotropically; the H atoms of the disordered Ph ring were not taken into account. The refinement converged to $wR_2 = 0.2131$ (on F^2_{hkl} for all 4579 reflections, 498 variables) with $R_1 = 0.080$ (on F_{hkl} for 2190 reflections with $I > 2\sigma(I)$). The highest peak in the final difference Fourier map had a height of 0.66 e Å^{-3}. The maximum negative peak in the final difference electron density synthesis was −0.43 e Å^{-3}. All calculations were performed on IBM PC with the help of the SHELXTL Plus 5 program [24]. Bond lengths and angles are listed in Table 1.

2.3. The NMR spectra

The ^{1}H-, ^{19}F- and ^{31}P-NMR spectra were recorded on a Bruker AMX-400 instrument. The operating frequencies were 400.13, 376.46 and 161.98 MHz, respectively. A 0.1 M solution in toluene-d_8 has been used. The fluorine chemical shifts (FCS) were measured relative to internal PhF; the plus sign corresponds to an upfield shift of the fluorine signal. The proton chemical shifts were determined relative to the residual signal of the methyl group of toluene (2.30 ppm). An ^{1}H thermometer based on the temperature-dependent shift difference between CH- and OH-protons has been used for temperature control. The method of measurement involved replacing the sample tube with a tube contain-

Table 2
The ^{19}F-NMR data for the solution of *trans*-(*o*-Tol)Ni(PEt_3)$_2$$N_3$($C_6H_4$F-4)$_2$ (**1**) in toluene-d_8

Temperature (K)	FCS (ppm) [a]	ΔFCS (Hz) [b]	$v_{1/2}$ (1) (Hz)	$v_{1/2}$(2) (Hz)	$v_{1/2}$(0) (Hz) [c]	$\tau_A \times 10^3$ (s) [d]
160	8.412; 10.490	781	56	50	29	
165	8.412; 10.483	779	51	47	26	
171	8.429; 10.499	778	34	33	22	12
181	8.450; 10.499	770	47	45	19	5.7
186	8.457; 10.503	769	58	56	17	3.9
191	8.481; 10.491	756	90	90	17	2.2
196	8.530; 10.451	722	155	162	16	1.05
			$r = 5.63$			
200	8.637; 10.330	628	302	282	15	0.69
			$r = 2.52$			
207	8.865; 10.160	478	$r = 1.93$ 15			
213	9.021; 9.982	368	226	227	15	
			$r = 2.39$			
223	9.101; 9.924	309	32	39	14	
			$r = 6.8$			
230	9.163; 9.901	277	18	18	14	
243	9.197; 9.879	256	16	16	12	
270	9.265; 9.850	220	14	14	11	
303	9.350; 9.811	173	10	10	5	
313	9.371; 9.801	162	9	11	5	
323	9.391; 9.788	149	12	13	5	
333	9.405; 9.772	138	19	25	5	
343	9.407; 9.740	125	41	53	5	
353	9.423; 9.700	104	$r_1 = 4.0$	$r_2 = 2.1$		

[a] The fluorine chemical shift relative to internal PhF, positive sign corresponds to upfield shift.
[b] The difference between FCS of two signals.
[c] The line width: $v_{1/2}$(1), left line; $v_{1/2}$(2), right line; $v_{1/2}$(0), PhF; *r*, ratio of main maximum to central minimum.
[d] The mean lifetime of fluorine in each site.

ing 4% methanol in CD_3OD for low temperatures or 80% 1,2-ethanediol in DMSO-d_6 for high temperatures.

2.4. Kinetic studies by dynamic NMR method

The mean lifetimes τ_A of the indicator nuclei in each site were calculated by using computer simulation for two-site exchange with unequal population [22]. Due to the fact that some temperature dependence of the differences $\Delta\nu^0$ between the frequencies of two sites in the absence of exchange was observed (see Tables 2 and 3), $\Delta\nu^0$ values near and above collapse were interpolated from low temperatures. In the case of ^{19}F-NMR spectra, the linewidth of internal PhF was chosen as the linewidth $\nu^0_{1/2}$ in the absence of exchange.

The thermodynamic activation parameters were calculated according to Arrhenius and Eyring equations. For the the reasons discussed below, it is possible to estimate correctly the τ_A values from the ^{19}F-NMR data only in the temperature range from -102 to -73°C. In fact only six points have been used for the calculation of the τ_A values. For ^{1}H-NMR spectra, it is possible to estimate the τ_A values (nine points) in the temperature range from -92 to -45°C. For ^{31}P-NMR spectra, eight points have been used for calculation of the τ_A values in the temperature range from -92 to -55°C. The errors in the thermodynamic parameters were determined by the usual procedure [25] taking into account the temperature range (29°C for ^{19}F, 37°C for ^{31}P and 47°C for ^{1}H) and are shown in Table 4.

3. Results and discussion

3.1. X-ray data

The structure of molecule 1 is shown in Fig. 1. The triazenide group in this complex acts as a monodentate ligand coordinating the Ni atom by only one of its nitrogen atoms. In fact, the Ni(1)···N(1) distance is as long as 2.797 Å and thus excludes the possibility of bonding interaction. The Ni(1) atom has a square-planar coordination geometry; the Ni–P and Ni–C (Ni(1)–P(1) 2.220(2) Å, Ni(1)–P(2) 2.221(2) Å, Ni(1)–C(25) 1.924(6) Å) bond lengths being close to their respective standard values (2.214 Å for Ni–PR_3, 1.917 Å for Ni–C(Ar) according to Ref. [26]). The mean planes of the *o*-tolyl and Ar–N_3–Ar ligands are approximately normal to the Ni atom coordination plane

Ni(1)P(1)P(2)N(3)C(25): the corresponding dihedral angles are equal to 91.3 and 93.7°, respectively. The Et groups of the PEt_3 ligands are in a staggered conformation with respect to each other.

The triazenide p-$FC_6H_4N_3C_6H_4F$-p ligand shows only small deviations from planarity, the largest displacement of the C(23) atom from the mean plane of the whole ligand being equal to 0.27 Å; the Ph ring

Table 3
The ^{1}H- and ^{31}P-NMR data for the solution of *trans*-(*o*-Tol)Ni(PEt_3)$_2$$N_3$($C_6H_4$F-4)$_2$ (**1**) in toluene-d_8

Temperature (K)	δ ^{1}H (ppm) [a]		$\tau_A \times 10^3$ (s) [b]	δ ^{31}P (ppm) [c]		$\tau_A \times 10^3$ (s) [d]
160	3.004	3.590		8.86	9.70	
	(23)	(18)		(22)	(21)	
165	3.018	3.580		8.84	9.64	
	(29)	(26)		(20)	(18)	
171	3.012	3.573		8.81	9.58	
	(28)	(23)		(28)	(20)	
176	3.026	3.564		8.74	9.50	
	(29)	(22)		(30)	(16)	
181	3.037	3.555	4.1	8.73	9.43	6.1
	(60)	(25)			(22)	
	$r_1 = 3.5$	$r_2 = 20$		$r_1 = 13.4$	$r_2 = 2.1$	
186	3.047	3.543	2.8	9.34		2.8
		(37)		(36)		
	$r_1 = 1.81$	$r_2 = 12$				
191	3.518		1.65	9.22		1.8
	(54)			(44)		
196	3.473		1.0	9.09		1.4
	(73)			(36)		
200	3.415		0.57	9.02		0.77
	(68)			(26)		
207	3.398		0.315	8.95		0.45
	(33)			(14)		
213	3.389		0.21	8.89		0.34
	(22)			(11)		
218	3.382		0.175	8.82		0.295
	(17)			(8.6)		
228	3.369		0.115	8.69		
	(11)			(6.6)		
243	3.349			8.48		
	(9)			(5.3)		
292	3.314			7.99		
	(7)			(5.2)		

[a] In parentheses, the line width; r_1, the ratio of the right maximum to the central minimum; r_2, the ratio of the left maximum to the central minimum.
[b] The mean lifetime of *o*-methyl protons in each site.
[c] From external H_3PO_4 at r.t.
[d] The mean lifetime of ^{31}P in each site.

Table 4
Thermodynamic parameters of dynamic processes for compounds **1** (present work) and **2** (from Ref. [22])

Compound	NMR	E_a (kcal mol^{-1})	$\Delta H^{\#}$ (kcal mol^{-1})	$\Delta S^{\#}$ (e.u.)	Temperature of coalescence (°C)	Temperature range of estimation of τ_A (°C)
1	^{19}F	6.8 ± 0.7	6.4 ± 0.7	-12 ± 3	[a]	-102 to -73
	^{1}H	6.7 ± 0.3	6.5 ± 0.3	-11 ± 1	-84	-92 to -45
	^{31}P	6.3 ± 0.4	6.0 ± 0.4	-13 ± 2	-88	-92 to -55
2	^{19}F	16.4 ± 0.4	15.7 ± 0.4	4 ± 2	63	25 to 80
	^{1}H	15.2 ± 0.8	14.6 ± 0.8	-1 ± 4	25	7 to 47
	^{31}P	[b]	[b]	[b]	10	

[a] Coalescence does not take place.
[b] Thermodynamic parameters in Ref. [22] have not been estimated due to small $\Delta\delta$°.

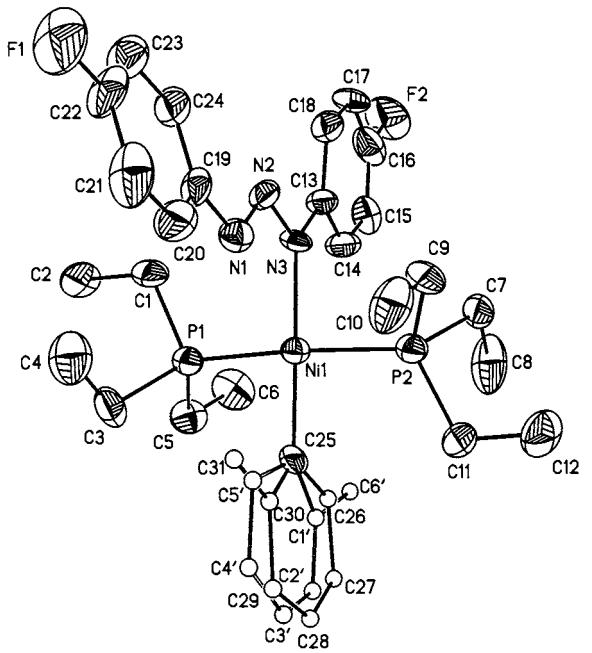

Fig. 1. Molecular structure of $Ni(PEt_3)_2(C_6H_4Me\text{-}2)(4\text{-}FC_6H_4N_3C_6H_4F\text{-}4)$ (**1**).

planes C(13)–C(18) and C(19)–C(24) are rotated by 8.7(7) and 16.1(7)° away from the plane of the central N_3 fragment. The N(1)–N(2) and N(2)–N(3) bond lengths (1.298(7) and 1.326(7) Å, respectively) are equal within 4σ, their average value (1.312 Å) being considerably larger than the standard value typical of the N=N bonds in azobenzene derivatives (1.255 Å [26]) and rather close to the delocalized N–N bond lengths (1.304 Å) normally observed in the aromatic pyridazine systems [26]. Thus, the bonds in the N–N=N fragment are delocalized and at least in part, involved in the conjugation with the Ph cycles. This is indicated by both the coplanarity of the Ph rings and the N_3 fragment and some shortening of the N–C(Ph) bonds, their average value 1.412 Å being about 0.02 Å shorter than the standard C(Ar)–N(=N) bond (1.431 Å as quoted in Ref. [26]). The difference between the individual N–N and C–N bonds (N(1)–N(2) versus N(2)–N(3) and N(1)–C(19) 1.403(8) Å versus N(3)–C(13) 1.421 Å) may be attributed to the influence of the metal atom which is coordinated only by the N(3) atom, whereas the N(1) atom is not involved in coordination (vide supra).

The detailed analysis of the difference Fourier maps suggested the disorder of the tolyl ligand, which was subsequently completely confirmed by the refinement of the disordered model. It turned out that the *o*-tolyl substituent in fact fills in two positions in crystal, which differ en grosse by a 180° rotation about the Ni–C bond. The somewhat different steric environments of the methyl group for each of the two orientations of the substituent obviously give rise to slight differences in the positions of the corresponding atoms of the tolyl ring within each of the components of the disorder. That is why it was possible to resolve the disorder for all phenylene ring carbon atoms with the exception of the C(25) *ipso*-atom, the disordered positions of which are still too close to each other and make the resolution absolutely impossible. Moreover, the careful refinement of the structure indicated that two components are not equally represented in the crystal, one of the positions (C(25)–C(31)) having about three times larger occupancy than its counterpart (C(1′)–C(6′)). Thus, the observed disorder allows us to treat the structure as a superposition of complexes with *cisoid* and *transoid* orientations of the $2\text{-}MeC_6H_4$ group with respect to the N(2)N(1)Ph fragment, the former compound appearing to be three times more abundant than the latter.

Previously, the structures of only two complexes of Ni(II) with the Ph–N_3–Ph fragments have been reported. One of them has a lantern-shaped $Ni_2(L)_4$ (L = PhN_3Ph) (**4**) molecule with the square-planar coordination of both Ni atoms and four bridging ligands each of them coordinating different Ni atoms by the N(1) and N(3) atoms [5]. The average Ni–N and N–N bond lengths (1.92(1) and 1.31(1) Å, respectively) are close to those found in the present structure. It is noteworthy, in particular, that in spite of the different functions of the ligands in the crystals of **1** and **4** and the involvement of two nitrogen atoms of each of the triazenide groups in metal coordination in the case of complex **4**, the N_3 systems in both complexes show almost the same degree of delocalization and are characterized by very similar geometric parameters.

Another previously studied complex $Ni_2(OH)_2(L')_2(L'')$ (**5**) [8] shows two types of three-nitrogen ligands (L′ = Ph–N_3H–C_6H_4–N_3H–Ph, L″ = Ph–N_3–C_6H_4–N_3–Ph) coordinated in two different ways. Each of the $–N^1{=}N^2{–}NH–$ fragments in each of the L′ ligands coordinates the Ni atom by one nitrogen atom (in the same way as in **1**), whereas each of the deprotonated $–N^1N^2N^3–$ fragments in L″ is chelating the Ni atom via its two nitrogens (N^1 and N^3) with the formation of the four-membered NiN_3 cycle:

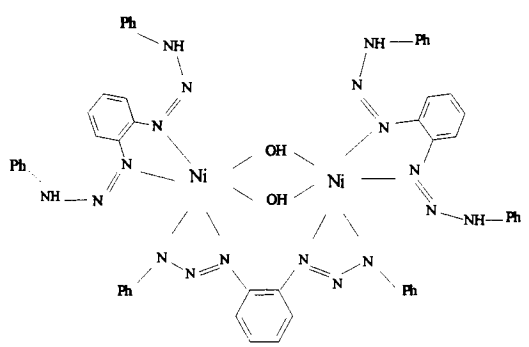

The similar pattern of N–N bond-length distribution is observed for all three ligands in **5** irrespective of the

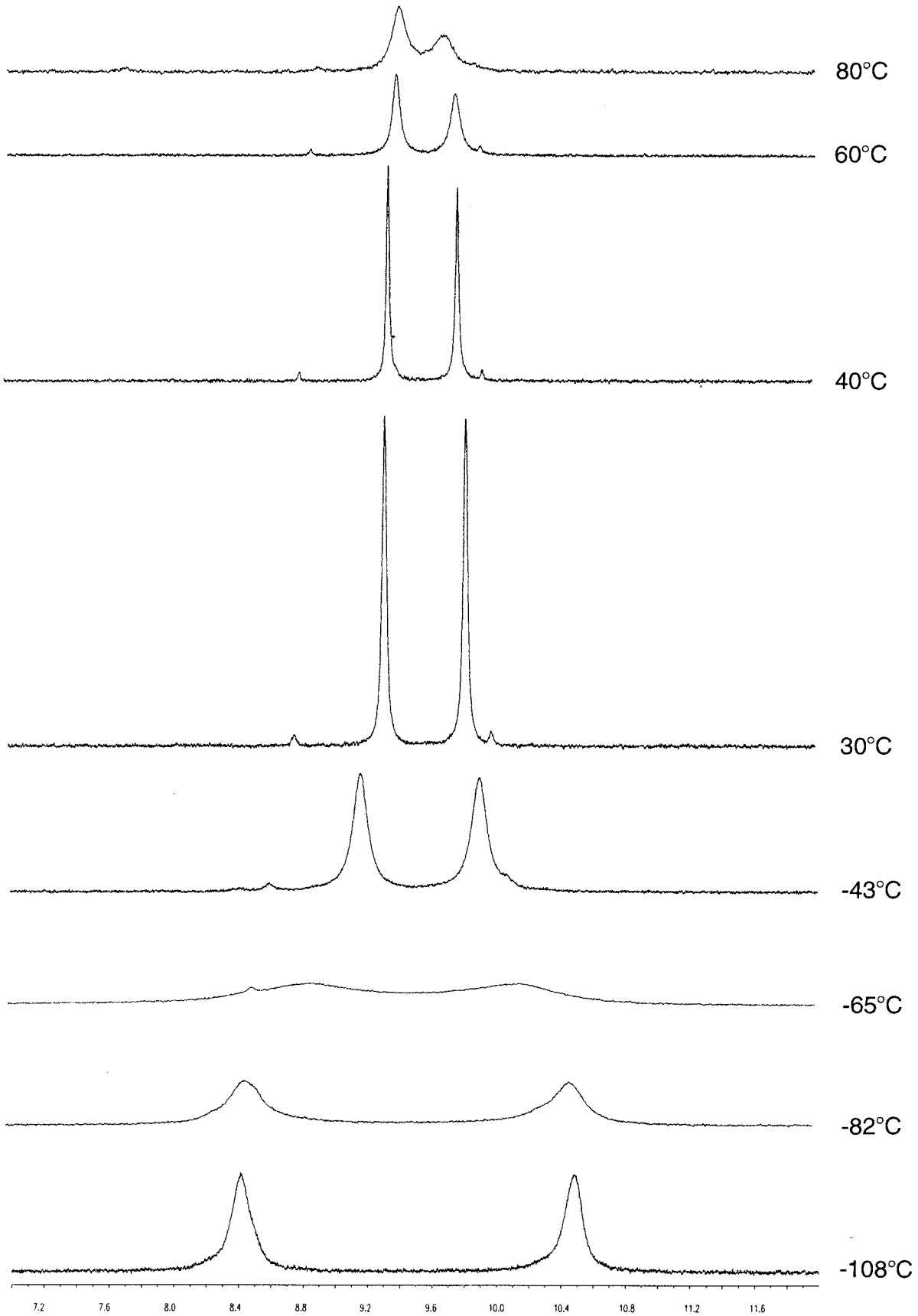

Fig. 2. The ^{19}F-NMR spectra of **1** at different temperatures (solution in toluene-d_8).

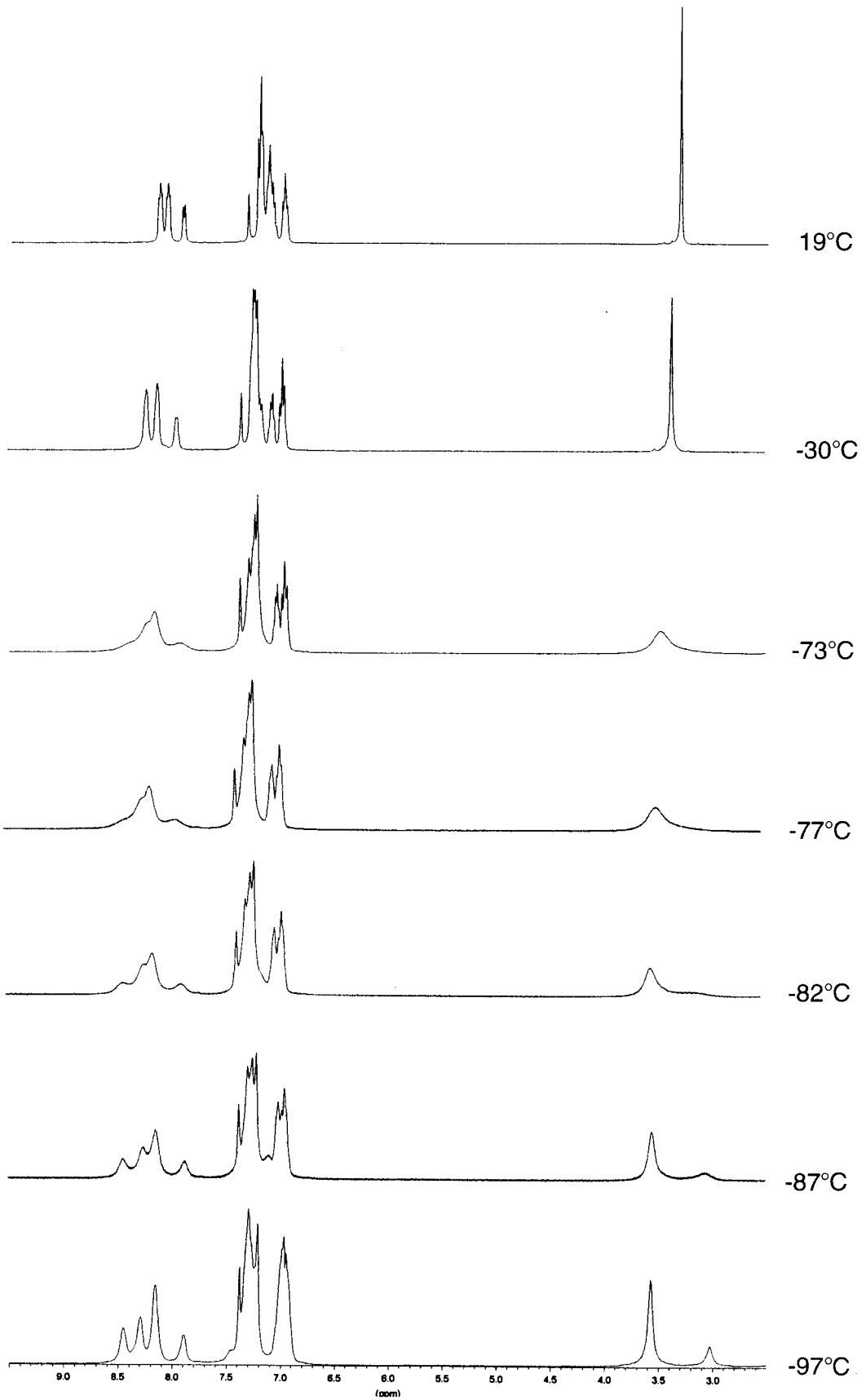

Fig. 3. The ^{1}H-NMR spectra of **1** at different temperatures (solution in toluene-d_8).

differences in their coordination modes. Specifically, one half of each ligand (H1) has equal N^1–N^2 and N^2–N^3 bonds (the average values are 1.325(7) and 1.313(7) Å, respectively), whereas the other half (H2) shows significant differences in these bonds (the corresponding average values are 1.342(7) and 1.271(7) Å). These two types of N–N bond delocalization may be accounted for by the difference in the strength of coordination with the nickel atom. Indeed, all Ni–N bonds involving the N atoms of the H1 half are noticeably shorter (2.050(6), 2.064(5), 2.084(6) and 2.123(6) Å) than the corresponding bonds with the N atoms of the H2 moiety (2.062(5), 2.091(6), 2.106(6) and 2.210(5) Å).

One may conclude that the distribution of the N–N bond lengths in the Ni-coordinated N_3–ligands depends neither on the form of the ligand (protonated or deprotonated) nor on the type of coordination and is rather determined by the redistribution of electron density in the coordination polyhedron of the nickel atom, manifested also in the differences between the Ni–N bond lengths.

3.2. NMR data

The ^{19}F-NMR data for compound **1** at different temperatures are given in Table 2. At −102°C there are two somewhat broadened fluorine signals with the difference in FCS (ΔFCS) equals to 2.07 ppm. These signals broaden upon increase of the temperature and almost collapse at −65°C (Fig. 2). Simultaneously some lowering of the ΔFCS value is observed. As the temperature is further increased, the fluorine signals contrary to the expectation do not collapse but at room temperature again become sharp and ΔFCS value equals to 0.47 ppm. On increasing the temperature above room temperature these signals broaden again and the ΔFCS value equals 0.32 ppm at 80°C.

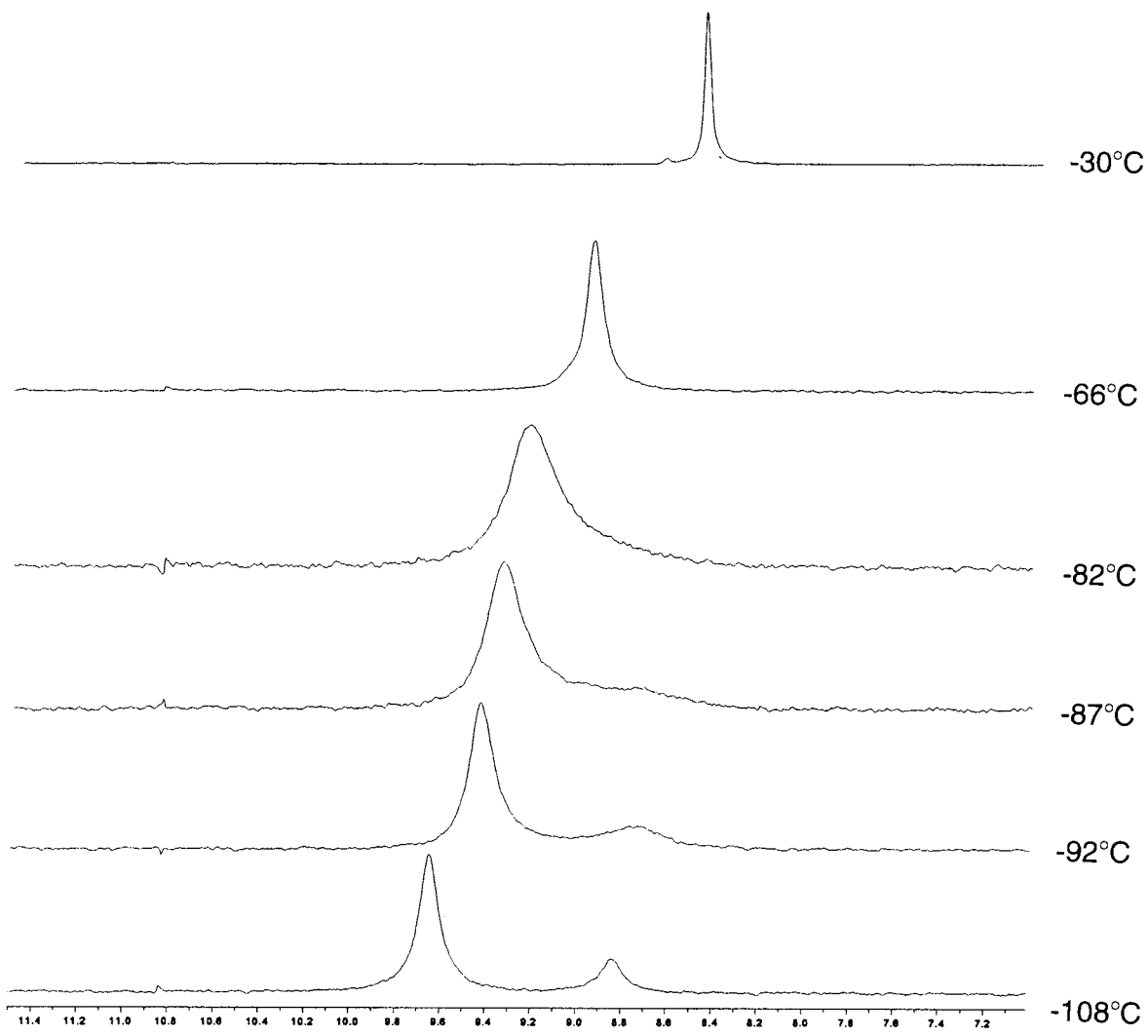

Fig. 4. The ^{31}P-NMR spectra of **1** at different temperatures (solution in toluene-d_8).

The ^{1}H- and ^{31}P-NMR data for compound **1** at different temperatures are given in Table 3. The ^{1}H-NMR spectrum of **1** at room temperature (Fig. 3) reveals one relatively sharp signal of protons from the *o*-methyl group. In the range 7.9–8.5 ppm, the signals of five aromatic protons are observed. The doublet at 7.9 ppm is *o*-hydrogen from *o*-Tol group. Four other signals correspond to the AA′ part of AA′BB′ pattern from two *p*-FC_6H_4 groups. On lowering the temperature the coalescence of aromatic protons is observed and at −97°C four broadened signals appear. The aromatic multiplets in the range of 6.9–7.4 ppm represent the superposition of other aromatic protons of compound **1**, of residual protons from toluene-d_8 and PhF added as internal standard for ^{19}F-NMR. The signal of protons of the *o*-Me group broadens and splits into two unequal (3:1) signals at −87°C. A similar behaviour is observed in the ^{31}P-NMR spectra (Fig. 4). One sharp signal of ^{31}P observed at room temperature broadens and splits into two unequal signals with the same ratio of intensities (3:1) on lowering the temperature below −92°C.

It should be noted that in all cases the spectral behaviour does not depend on concentration (from 0.03 to 0.1 M) and is completely reversible with respect to temperature changes.

Before discussing the results obtained for nickel complex **1**, it should be noted that in the case of the related Pt complex **2** somewhat different spectral behaviour has been found in ^{19}F-NMR spectrum [22]. Thus in the spectra of **2** two sets of sharp fluorine signals at 8 and 11 ppm are observed already at 0°C. The coalescence of these signals takes place at 63°C and at higher temperatures the broad singlet begins to narrow up to 80°C. In general the spectral pattern is typical for usual dynamic spectra and was explained by the intramolecular migration of (*o*-Tol)Pt(PEt_3)$_2$ group, which is accelerated on increasing the temperature and leads to the averaging of fluorine shielding. For Ni complex **1** the normal spectral pattern, which may be explained in the context of the tautomeric process:

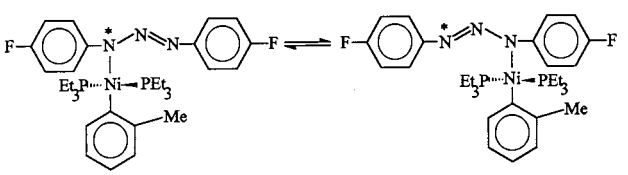

is observed at substantially lower temperature. At −113°C the migration is slow (two separated fluorine signals with large ΔFCS = 2.08 ppm). On increasing the temperature up to −60°C, the spectral pattern becomes consistent with the pattern that is expected for acceleration of migration. The following thermodynamic parameters were found for this process: $E_a = 6.8 \pm 0.7$ kcal mol^{-1}, $\Delta H^{\#} = 6.4 \pm 0.7$ kcal mol^{-1}, $\Delta S^{\#} = -12 \pm 3$ e.u. The comparison of these thermodynamic parameters with the corresponding values for Pt complex **2** ($E_a = 16.4 \pm 0.4$ kcal mol^{-1}, $\Delta H^{\#} = 15.7 \pm 0.4$ kcal mol^{-1}, $\Delta E^{\#} = 4 \pm 2$ e.u.) allows us to make the conclusion that the migration of ML_n group proceeds with considerably smaller activation barrier in the case of M = Ni than for M = Pt. At the same time, the negative change of activation entropy is observed in the case of **1** and the small positive change of activation entropy is observed in the case of **2**.

The ^{19}F-NMR spectra of **1** at the temperature as high as −60°C suggest that the rate of the migration decreases on increasing the temperature. It should be emphasized that a strong decrease of ΔFCS value is simultaneously observed. Moreover, in temperature range −40 to +70°C a very good correlation of ΔFCS value and T are observed (ΔFCS = $-1.357T + 587$; $r = 0.999$; $s = 2.8$). Taking into account that the FCS value of 4-fluorophenyl group is the indicator of electron density on the adjacent atom [27,28], the last fact may indicate the decrease in the difference between electron density on N(1) and N(3) atoms on increasing the temperature. It may be suggested that at elevated temperatures the conformation of *S-trans* type is stabilized:

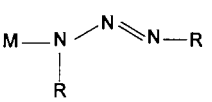

Such conformation is characterized by a higher degree of coplanarity of Ni–N(3) and N(1)–N(2) bonds and better conjugation between the N(3) lone electron pairs and the N=N bond. At the same time, this conformation hinders the intramolecular migration of organometallic group, which may be realized only in the *S-cis*-conformation.

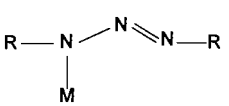

In discussion of the ^{1}H- and ^{31}P-NMR data obtained at different temperatures, it should be noted that spectra in Figs. 3 and 4 are also different from corresponding spectra for Pt compound **2**. In particular, the splitting of proton signals of *o*-methyl group and of phosphorus signals in two signals for Ni compound **1** (−84 and −88°C) takes place at substantially lower temperatures than for Pt complex **2** (25 and 10°C). Moreover, the ratio of integral intensities of signals for **1** (3:1) is higher than the corresponding ratio (1.4:1) for **2**.

In the previous paper [22], we have suggested that one of the reasons for the splitting of corresponding signals in ^{1}H- and ^{31}P-NMR spectra of Pt complex **2** may be the hindered rotation around the N(2)–N(3) bond:

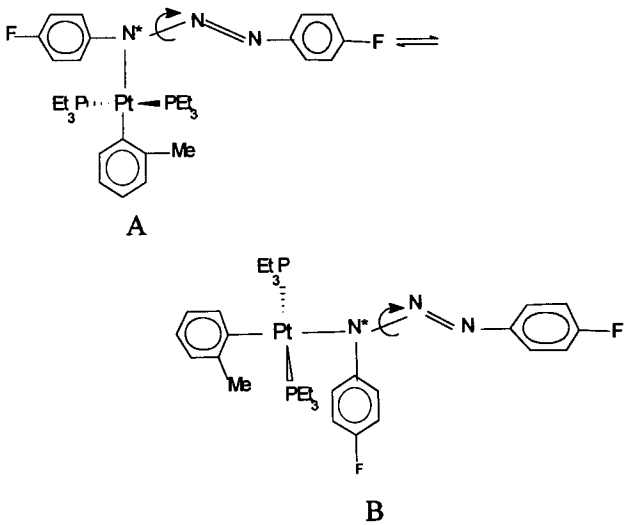

and the existence of two conformers A and B, in which the *o*-methyl protons or ^{31}P nuclei of PEt_3 ligands may be magnetically nonequivalent. The similar explanation may be suggested for the interpretation of ^{1}H- and ^{31}P-NMR data for Ni complex **1**:

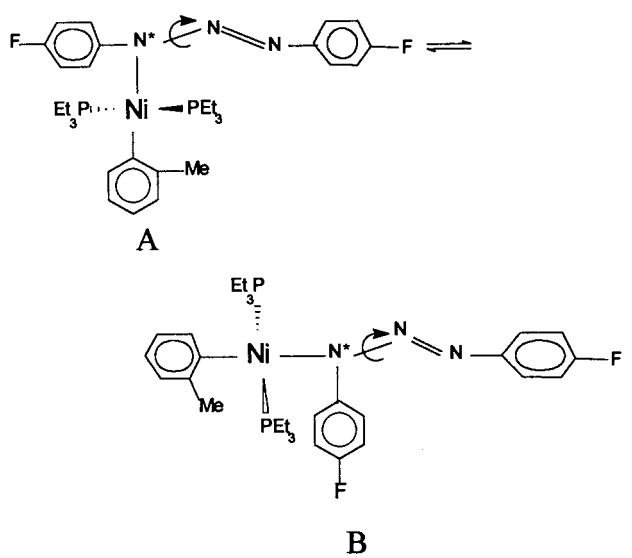

The increase in the ratio A/B in going from compound **2** to compound **1** may be caused by the shorter Ni–N(3) bond in comparison with the Pt–N(3) bond. The thermodynamic parameters calculated from ^{1}H- and ^{31}P-NMR spectra for possible A⇔B transformation in compound **1** as well as in Pt compound **2** are given in Table 4. It follows from these data that the possible A⇔B transformation as well as the migration of ML_n group have a considerably lower activation barrier for Ni compound **1** than for Pt compound **2**.

It should be noted that in general ^{1}H-NMR spectra of Ni complex **1** may be complicated by the possible existence of additional isomers for A as well as for B, due to the hindered rotation around Ni–N(3) and/or Ni–C bonds. For example, the hindered rotation around Ni–C bonds causes the existence of a mixture of *syn*- and *anti*-isomers in *trans*-$(o\text{-Tol})_2Ni[P(Me)_2Ph]_2$ [29]. In our situation magnetic non-equivalence may also be observed, even in the case of the existence of the only conformer A, and is not necessarily connected with the existence of conformer B. However, in this case the shielding of phosphorus nuclei of two PEt_3 ligands in the coordination plane, which is orthogonal on the one hand to the Ni–N(3)–N(2)=N(1) plane and on the other hand to the *o*-Tol ligand plane, should not be different in the first approximation. This, however, is not consistent with the experimental data. The magnetic non-equivalence of ^{31}P nuclei observed for Pt complex **2** was the basic evidence in favour of the existence of two conformers A and B.

At the same time, according to X-ray data obtained in the present paper, complex **1** in the crystalline state exists as the 3:1 mixture of two isomeric complexes with *cisoid* and *transoid* orientation of the *o*-methyl group relative to the N(2)=N(1) bond. It should be noted that in the ^{1}H- and ^{31}P-NMR spectra of compound **1** at low temperatures, we observed the same ratio (3:1) of intensities of corresponding signals of indicator nuclei. Moreover, according to the X-ray structure of compound **1**, it is actually the C–N–N=N–C

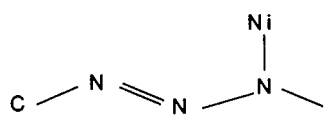

rather than the Ni–N–N=N–C chain which shows a zig–zag conformation. Italian authors have observed a similar structure for triazenido complexes of Pd and Pt [10,12,13].

It should be emphasized that the tautomeric process in the case of the migration of the $(o\text{-Tol})M(PEt_3)_2$-group implies transformation of two isomers C and D:

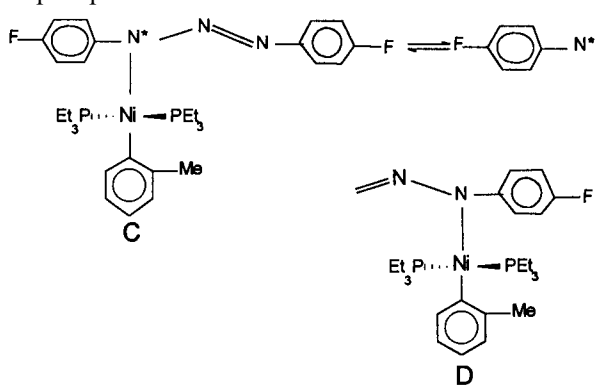

in which the shielding of *o*-Me protons must be different. In the context of our discussion it is important to take into account the fact that, in principle small deviations from the orthogonality of planes N–N=N, *o*-Tol and coordination plane of Ni may be sufficient for causing the magnetic nonequivalence of ^{31}P nuclei to be observed in ^{31}P-NMR spectra. The existence of such a small deviation follows from our X-ray data. More-

over, it should be pointed out that the close values of activation parameters obtained in the present paper from dynamic ^{19}F-, ^{31}P- and ^{1}H-NMR spectra for Ni compound **1** as well as previously from ^{19}F- and ^{1}H-NMR spectra of Pt compound **2** (Table 4).

In this connection, it should be once more emphasized that the dynamic ^{19}F-NMR spectra of compounds **1** and **2** with a large difference in fluorine shielding of the indicator 4-FC_6H_4 groups undoubtedly reflect the migration of the ML_n group. It should also be noted that the close thermodynamic characteristics obtained from dynamic ^{1}H-, ^{31}P- and ^{19}F-NMR spectra may also be explained if it is assumed that A⇔B transformation is the rate-determining stage of the tautomeric process.

4. Conclusions

The dynamic NMR spectra of the triazenido complex of nickel(II) (**1**) suggest that the migration of (*o*-Tol)Ni(PEt_3)$_2$ group occurs at low temperatures in solution. This migration implies the interconversion of two isomers with *cisoid* or *transoid* orientation of the *o*-Me group relative to the N(2)=N(1) bond. The interconversion becomes slow at elevated temperatures due to the rotation processes. In solid state, complex **1** exists as a 3:1 mixture of above isomers.

5. Supplementary material

Crystallographic data for the structural analysis have been deposited with the Cambridge Crystallographic Data Centre, CCDC no. 117228 for compound **1**. Copies of this information may be obtained free of charge from The Director, CCDC, 12, Union Road, Cambridge CB2 1EZ, UK (Fax: +44-1223-336033 or e-mail: deposit@ccdc.cam.ac.uk or http://www.ccdc.cam.ac.uk).

Acknowledgements

The authors are indebted to the Russian Foundation for Basic Research for financial support (Project No. 97-03-33783) and for covering the License Fee for the use of the Cambridge Structural Database, which was employed for the analysis of the structural results discussed in the present paper (Project No. 96-07-89187).

References

[1] F.P. Dwyer, J. Am. Chem. Soc. 63 (1941) 78.
[2] C.M. Harris, B.F. Hoskins, R.L. Martin, J. Chem. Soc. (1959) 3728.
[3] L. Toniolo, T. Boschi, G. Deganello, J. Organomet. Chem. 93 (1975) 495.
[4] M. Corbett, B.F. Hoskins, J. Am. Chem. Soc. 89 (1967) 1530.
[5] M. Corbett, B.F. Hoskins, N.J. McLeod, B.P. O'Day, Austr. J. Chem. 28 (1975) 2377.
[6] W.H. Knoth, Inorg. Chem. 12 (1973) 38.
[7] M. Corbett, B.F. Hoskins, J. Chem. Soc. Chem. Commun. (1968) 1602.
[8] M. Horner, H. Fenner, W. Hiller, J. Beck, Z. Naturforsh. Teil B 43 (1988) 1174.
[9] J.V. Cuevas, C. Garsia-Herbosa, M.A. Munoz, S.W. Hickman, A.G. Orpen, N.G. Connelly, J. Chem. Soc. Dalton Trans. (1995) 4127.
[10] G. Bombieri, A. Immirzi, L. Toniolo, Trans. Met. Chem. 1 (1976) 130.
[11] J. Bailey, V.J. Catalano, H.B. Gray, Acta Crystallogr., Sect. C 49 (1993) 1598.
[12] A. Immirzi, G. Bombieri, L. Toniolo, J. Organomet. Chem. 118 (1976) 355.
[13] L. Taniolo, A. Immirzi, U. Croatto, G. Bombieri, Inorg. Chim. Acta 19 (1976) 209.
[14] K.R. Laing, S.D. Robinson, M.F. Uttley, J. Chem. Soc. Dalton Trans. (1974) 1205.
[15] L.D. Brown, J.A. Ibers, Inorg. Chem. 15 (1976) 2794.
[16] C.J. Creswell, M. Queiros, S.D. Robinson, Inorg. Chim. Acta 60 (1982) 157.
[17] E.V. Borisov, A.S. Peregudov, S.A. Postovoi, E.I. Fedin, D.N. Kravtsov, Izv. Akad. Nauk. Ser. Khim. (1986) 550.
[18] A.N. Nesmeyanov, E.V. Borisov, A.S. Peregudov, D.N. Kravtsov, L.A. Fedorov, E.I. Fedin, S.A. Postovoi, Dokl. Acad. Sci. USSR 247 (1979) 1154.
[19] D.N. Kravtsov, A.N. Nesmeyanov, L.A. Fedorov, E.I. Fedin, A.S. Peregudov, E.V. Borisov, P.O. Okulevich, S.A. Postovoi, Dokl. Acad. Sci. USSR 242 (1978) 347.
[20] P. Peringer, Inorg. Nucl. Chem. Lett. 16 (1980) 461.
[21] A.S. Peregudov, Dissertation, 1993, Moscow.
[22] A.S. Peregudov, D.N. Kravtsov, G.I. Drogunova, I.A. Godovikov, Inorg. Chim. Acta 280 (1998) 238.
[23] D.C. Morreli, J.K. Kochi, J. Am. Chem. Soc. 96 (1975) 7262.
[24] G.M. Sheldrik, SHELXTL Version 5.0, Software Reference Manual, Siemens Industrial Automation, Madison, WI, 1994.
[25] J. Sandsrom, Dynamic NMR Spectroscopy, Academic, London, 1982.
[26] H.-B. Bürgi, J.D. Dunitz (Ed.), Structure Correlation, vol. 2, VCH, Weinheim, New York, 1994, p. 767.
[27] N.A. Ogorodnikova, A.S. Peregudov, E.I. Fedin, D.N. Kravtsov, Bull. Acad. Sci. 38 (1989) 2037.
[28] D.N. Kravtsov, A.S. Peregudov, O.B. Sherbakova, Yu. A. Borisov, Russ. Chem. Bull. 44 (1995) 1841.
[29] K. Miki, M. Tanaka, N. Kasai, M. Wada, J. Organomet. Chem. 352 (1988) 385.